Molecular Crystals and Liquid Crystals
Publication details, including instructions for authors and subscription information:
http://www.tandfonline.com/loi/gmcl16

The Critical Pitch-Thickness Relation at the Cholesteric-Nematic Phase Transition by the Optical Mass Transport Method

H. Hakemi [a b]

[a] Department of Chemistry, Gross Chemical Laboratory, Duke University, Durham, NC, 27706

[b] S.C. Johnson & Son, Inc., Corporate Research, Racine, WI53403

Version of record first published: 20 Apr 2011.

To cite this article: H. Hakemi (1985): The Critical Pitch-Thickness Relation at the Cholesteric-Nematic Phase Transition by the Optical Mass Transport Method, Molecular Crystals and Liquid Crystals, 116:3-4, 285-297

To link to this article: http://dx.doi.org/10.1080/00268948508074579

Mol. Cryst. Liq. Cryst., 1985, Vol. 116, pp. 285–297
0026-8941/85/1164–0285/$20.00/0

Printed in the United States of America

The Critical Pitch-Thickness Relation at the Cholesteric-Nematic Phase Transition by the Optical Mass Transport Method

H. HAKEMI†

Department of Chemistry, Gross Chemical Laboratory, Duke University, Durham, NC 27706

(*Received June 15, 1984*)

The optical mass transport (OMT) method was utilized to study the cholesteric pitch as a function of thickness at the cholesteric-nematic phase transition in a wedge-type diffusion cell at two different geometries. We obtained a linear relation between the cholesteric finger print pitch (P_c) and the film thickness (L_c) at the critical cholesteric-nematic boundary layer. The measurements were done by direct observation via an optical microscope. Due to the presence of the concentration gradient, the surface anchoring is weakened and large pitch values within the range of $L_c/P_c \lesssim 0.15$ were established. The thickness gradient as well as the concentration gradient showed systematic linear effects on the data. We found a qualitative agreement between the present experimental data and that of a previous theory.

INTRODUCTION

Field induced cholesteric-nematic phase transition is a well known phenomenon in the liquid crystal. This has led to interesting electro-optical properties in display and addressing technology. The cholesteric-nematic transition induced by external fields was first treated theoretically by de Gennes[1] and Meyer[2] and has been observed experimentally by Wysoki, Adams and Haas[3] by the application of the electric field.

The undulation of the cholesteric helix at the cholesteric nematic transition depends not only on the sign of the dielectric anisotropy, the diamagnetic susceptibility and the direction and intensity of the applied external forces, but also depends on the type of the surface treatment and the strength of the liquid crystal-surface interactions.

†Present Address: S.C. Johnson & Son, Inc., Corporate Research, Racine WI 53403.

In the absence of the external field, the influence of the surface anchoring may be so important that it can determine the instability and dilation of the cholesteric structure, resulting into a cholesteric-nematic phase transition. These surface effects are particularly important when the sample thickness is comparable with or smaller than the pitch of the cholesteric helix and surfaces have been treated to give homeotropic (perpendicular) alignment. The homeotropic boundary condition (in which helix axis is parallel to surfaces) are not compatible with a regular, uniform planar texture (formation with helix axis perpendicular to surfaces) and if the sample is thin enough, the boundary conditions dominate and a cholesteric-nematic phase transition is observed. The boundary induced cholesteric-nematic transition of long pitch cholesteric liquid crystals with homeotropic alignment has been reported by Harvey.[4] It has been shown that in a uniformly concentrated cholesteric mixture under a thickness gradient, the undulation of the cholesteric pitch would occur at sample thicknesses comparable with the undisturbed pitch values. This author has not reported the relation between the critical thickness (at the cholesteric-nematic transition) and the value of the disturbed (storage mode or finger-print) pitch, observed directly at the phase transition. The ratio between the undisturbed pitch value obtained by cano wedge method and the tilted pitch value from the finger-print texture at the critical thickness should be directly proportional to the surface boundary effect. The relation between the degree of the tilt of the cholesteric pitch and the strength of the surface anchoring has not yet been verified quantitatively.

In general, the surface forces act strongly on the long-pitch and weakly on the short-pitch cholesterics. In the small thickness-to-pitch ratios; e.g. $L/p < 0.2$, if the homeotropic surface anchoring is strong, the nematic phase is usually stable (i.e. cholesteric-nematic transition occurs), whereas for weak surface anchoring a well defined cholesteric finger print is established.[5-10]

The theoretical treatment of the cholesteric storage mode (finger print) to the nematic phase in critical restricted geometries has shown that in the vicinity of the critical thickness the cholesteric pitch diverges as a logarithmic function and by decreasing the plate spacing (film thickness) to a critical value, the system becomes nematic.[11] The experimental verification of this theory has not yet been reported.

The aim of the present work is to report a preliminary experimental results on the relation between the critical cholesteric finger print and the film thickness at the cholesteric-nematic phase transition induced by the surface effect. The surface induced phase transition is established by the diffusion study via the optical mass transport

(OMT) technique. The experimental details of this method has been mentioned elsewhere.[12] According to OMT method, when a cholesteric, or generally an optically active species, is allowed to diffuse into a uniaxially oriented homeotropic nematic thin film, the diffusion profile, consisting of a mass distribution resulting from the concentration gradient driving force, could be observed microscopically by the measurable cholesteric pitch gradient texture. The space and time analysis of such a texture has provided valuable data on the diffusion coefficients in these systems.[12,13,14]

In a typical diffusion profile with homeotropic alignment, the effect of the surface interactions is to provide a distinct cholesteric-nematic phase transition boundary with the largest pitch value (lowest concentration) at the diffusion front (See figure (2)). The critical cholesteric pitch value at this boundary layer remains constant during the diffusion process as long as the film thickness is uniform. Therefore, at constant temperature and pressure, there is a direct and spontaneous correlation between the critical pitch; P_c and its corresponding surface geometry or film thickness; L_c. In the present study, we used diffusion cells with thickness gradient to provide a condition for investigating the characteristics of the pitch-thickness relation at the cholesteric-nematic phase transition boundary layer. Depending upon the direction of the thickness gradient; ∇L, with respect to the diffusion mass flux $\vec{J}$, the critical pitch-thickness relation was obtained from either space or time analysis of the diffusion profile. The details of the diffusion experiment at non-uniform thickness and the method of pitch-thickness evaluation at the two corresponding geometrical boundary conditions are mentioned in section II. In section III we give our experimental data on the critical pitch-thickness relation at the cholesteric-nematic boundary and study the effects of the thickness gradient and concentration gradient on these results. Comparison of our data with the available theoretical prediction gives a qualitative agreement. The quantitative testing of the theory would however require further knowledge on the material constants such as; the values of elastic constants and the surface energy coefficient of the system.

(II) EXPERIMENTAL

1. General

The liquid crystalline materials used in the diffusion study are; a) cholesteryl-(R)-2 methyl valerate (R–CMV), which is utilized as an

optically active diffsant and b) 4-methoxy-benzylidene-4′-n-butylaniline (MBBA), as the nematic matrix. The synthetic procedure and thermal properties of R–CMV, which has a monotropic smectic-A phase transition, has been described elsewhere.[15,16] The nematic MBBA was obtained from Eastman Kodak and used without further purification.

The diffusion cell was prepared by placing the nematic MBBA between a pair of lecithin coated microscope slides providing a uniaxial homeotropic orientation. The diffusion profile was established by allowing an infinitesimal amount of a 4% (w/w) solution of R–CMV/MBBA to diffuse linearly into the MBBA nematic matrix at the ambient temperature of 25°C. The direction of the mass flux $\vec{J}$ is always perpendicular to that of the homeotropic alignment of the nematic director $\vec{n}$ (see figure (1)). The continuous variation of the film thickness was accomplished by using mylar spacers with two different thicknesses at the corresponding ends of the diffusion cells. According to the relative direction of the thickness gradient; ∇L, to that of the mass flux $\vec{J}$, two orthogonal geometries are established as: (1) $\vec{J} \| \nabla L$ and (2) $\vec{J} \perp \nabla L$. The schematic diagrams of these geometries are represented in figure (1). According to the schematic diagram of geometry (1), it is evident that two diffusion conditions of $\vec{J}\|$ $(+\nabla L)$ and $\vec{J}\|$ $(-\nabla L)$ may prevail. However, the present experimental study only concerns the latter condition as the geometry (1). Notice that in all experiments, the original direction of the nematic director $\vec{n}$ is perpendicular to both $\vec{J}$ and ∇L, whereas the

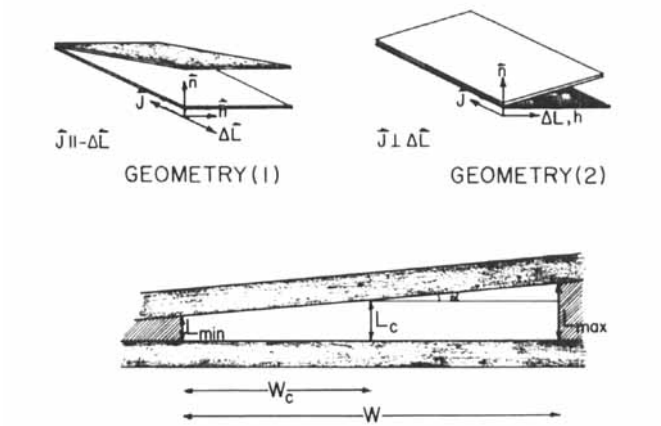

FIGURE 1 The experimental boundary conditions and parameters of the diffusion geometries (1) and (2).

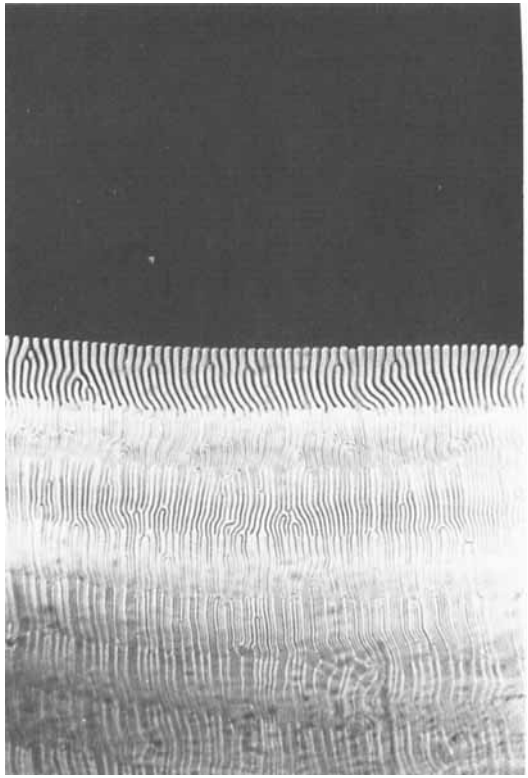

FIGURE 2 The diffusion profile of R-CMV/MBBA system in the geometry (1) under crossed polars (68X).

average directions of the cholesteric helix axis are; $\vec{h} \perp \vec{J}$ in geometry (1) and $\vec{h} \parallel \vec{J}$ in geometry (2).

According to the nature of the diffusion boundary conditions in the geometry (1), the relation between the critical pitch; P_c and its corresponding thickness; L_c must be obtained from the time analysis of the diffusion profile. In figure (2) we show a photomicrograph of the diffusion profile at a time from which one data point for P_c–L_c relation may be determined. In the geometry (2), however, the space analysis of the continuously varying P_c will provide the total range of the P_c–L_c relationship. Figure (3) represents a photomicrograph of the typical critical pitch variation across the diffusion front as a function of the critical thickness.

The determination of the apparent critical P_c values in either geometries (1) or (2) are done from the measurement of the periodicity

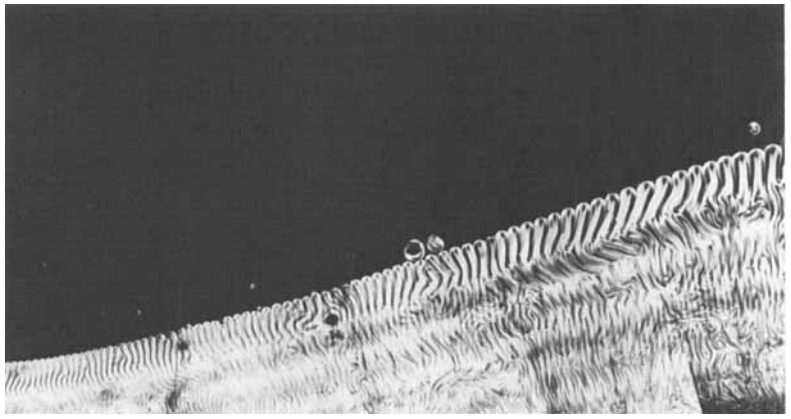

FIGURE 3 The diffusion profile of R-CMV/MBBA system in the geometry (2) under crossed polars (68X).

of the successive observed retardations; S_c at cholesteric-nematic boundary from the relation; $P_c = 2S_c$. The corresponding L_c values are evaluated from the relation;

$$L_c = \frac{W_c}{W}(L_{\max} - L_{\min}) + L_{\min} \tag{1}$$

where $L_{\min}$ and $L_{\max}$ are the minimum and maximum values of the plate spacing, W the width of the wedge and W_c the distance of the corresponding p_c value from the thinner side of the thickness gradient. These parameters are described in figure (1). From the equation (1), the gradient of the film is described by; $\tan(\alpha) = [(L_{\max} - L_{\min})/W]$. Notice that in the diffusion profile of geometry (2), since the diffusion front is tilted with respect to the source, the necessary modification of the wedge angle α, and correction of L_c values has to be the considered. The pitch and thickness measurements were performed under an LKE Nickon polarization microscope equipped with an optical micrometer and a polaroid camera.

(III) RESULTS AND DISCUSSIONS

A) Critical pitch-thickness relation:

In figure (4) we present the experimental results of the critical pitch-thickness relation (P_c vs L_c plots) at the two geometries (1) and (2).

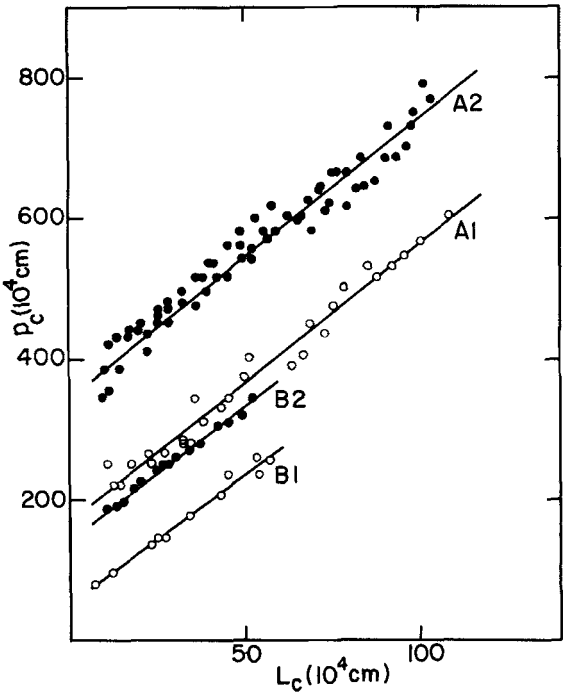

FIGURE 4 The critical pitch (P_c) - thickness (L_c) relation in geometry (1) (dark circles) and geometry (2) (open circles) at different thickness gradients. See table (I) for the curve notations.

In each geometry, the diffusion profiles were prepared at two different thickness gradients by only varying the larger end of the wedge spacer. The experimental parameters of these geometrical boundary conditions are tabulated in Table (I). The data at larger thickness gradients in each geometry, which are denoted as experiments A1 and A2, are obtained from three independent diffusion studies. Whereas, those at the smaller thickness gradients, denoted as B1 and B2, were acquired from a single diffusion experiment.

From the data of figure (4), we find that P_c–L_c relation is dependent on both geometrical boundary condition and the thickness gradient. However, regardless of the above contributing effects, the general characteristics of the plots are predominately linear and within the first order approximation may be represented by the following phenomenological relation:

$$p_c = p_c^\circ + \beta L_c \tag{2}$$

TABLE I

Geometrical Parameters and Boundary Conditions of the Diffusion Study in R–CMV/MBBA System.

Geometry	Experiment	(104 cm)		(cm)	(10^3)	(10^4 cm)	
		L_{min}	L_{max}	W	tan (α)	P_c°	β
(1) $\vec{J} \parallel (-\nabla\vec{L})$	A1	6.5	108	0.725	14.5	195	3.9
	B1	6.5	58	0.660	7.8	75	3.7
(2) $\vec{J} \perp \nabla\vec{L}$	A2	6.5	108	0.680	15.0	370	3.9
	B2	6.5	58	0.635	8.1	165	3.8

where P_c° is the apparent critical pitch value at the minimum experimental thickness limit, i.e. $L_{\min} = 6.5 \times 10^{-4}$ cm and β, the proportionality factor, is the linear phenomenological slope of the P_c–L_c plots. We found that in the present R–CMV/MBBA, β is independent of the type of geometry or the thickness gradient and exhibit an average constant value of 3.8 ± 0.1. The value and constancy of β must, hence, represent a measure of the material constants of the chemical components in the system and the nature and strength of the liquid crystal-surface interactions.

B) Effect of the thickness gradient:

The effect of the thickness gradient; ∇L on the P_c–L_c plots can be found by comparing the data at the same geometry with two different ∇L values. It is evident that the larger the thickness gradient the larger is the displayed pitch value, when measured at a constant thickness. The direct proportionality between ∇L and P_c in either geometry (figure (4)) is a manifestation of the surface anchoring effect on stabilizing the cholesteric pitch. Obviously by increasing the thickness gradient, the liquid crystal-surface interactions is diminished which would cause the larger P_c values at the cholesteric-nematic transition to be stable. This conclusion may be further confirmed from the data of figure (5) in which all P_c values (in either geometry) are normalized against the corresponding thickness gradient by dividing into tan (α). The plots of $P_o/\tan(\alpha)$ vs L_c in each geometry are basically following the same curve. In this figure, the experiments B1 and B2 exhibit slightly sharper slopes than those of A1 and A2, respectively. The source of this difference which cannot be singled out in the present work is most likely due to non-linear effect of the thickness gradient and, therefore, the effect of surface anchoring on the stability of the cholesteric fingerprint structure.

C) Effect of diffusion geometry and concentration gradient:

Regardless of the thickness gradient effect, when the data of figure (5) at the two geometries are compared, it becomes evident that the difference between the data in geometry (1) and (2) must predominantly arise from the inherent difference in the manifestation of the cholesteric pitch between the time-frame and space-frame of the diffusion profile. More specifically, in geometry (1) where the concentration and thickness gradients are parallel, the apparent critical pitch values are smaller than those in the geometry (2), in which concentration and thickness gradients are orthogonal. The origin of this

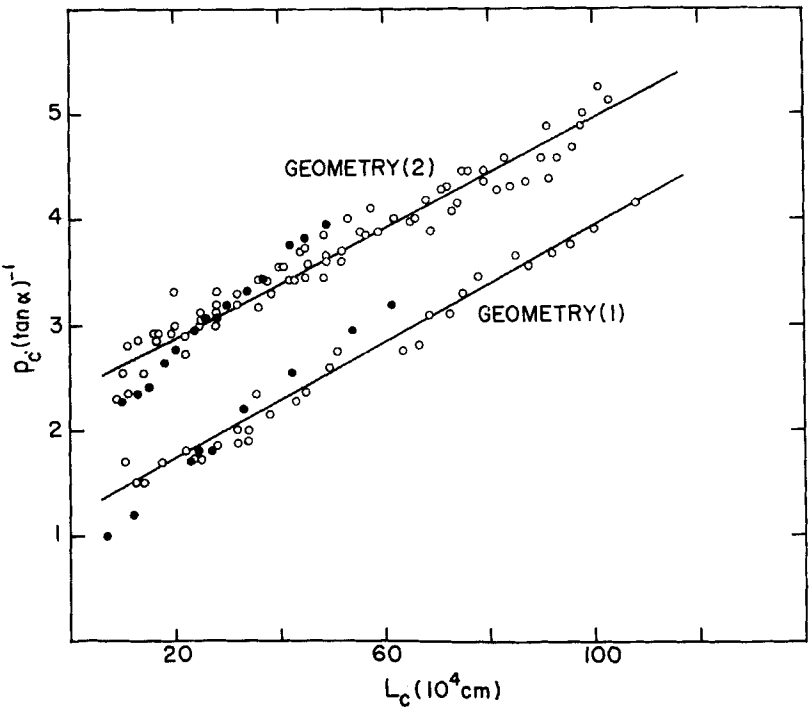

FIGURE 5 The relation between the critical normalized pitch (P_c/tan (α)) and the thickness (L_c) in the two geometries. Open circles: experiments A1 and A2. Dark circle: experiments B1 and B2.

seemingly non-ergodic behaviour may rest on the effect of the diffusion concentration gradient on the liquid crystal-surface interactions. Notice that in the case of the ergodic behaviour, all data in figure (5) are expected to fall on the same curve. In other words, P_c in the time-frame experiment (geometry(1)) is less influenced by the surface anchoring and, therefore, more influenced by the concentration gradient than in space-frame experiment (geometry (2)). The quantitative verification of this result has yet to be attempted and requires the consideration of the other experimental alternative (i.e.; use of the boundary condition; $\vec{J} \parallel (+\nabla L)$ in the geometry (1)).

Other important aspect of the effect of the concentration gradient on the surface interaction energy, and consequently on the P_c–L_c relation, is the small range of L_c/P_c ratio from the diffusion experiments. In the present study we found that $L_c/P_c \lesssim 0.1$, whereas in the wedge-type cell at uniform concentration reported by Havery,[4] this ratio was; $L_c/P_c \approx 1.0$. The pitch values reported by the above

author have been determined from the planar texture by the Cano-Wedge technique.[17] This represents values of the undisturbed pitch. Although no attempts have been made to report the apparent pitch (P_c in this study) values from a microscopic analysis, our estimate from figure (1) of reference (4) shows that the estimated P_c value are approximately the same as the undisturbed pitch value from Cano-Wedge method. Hinov *et al.*[10] reported the establishment of large cholesteric fingerprint texture with $L_c/P_c < 0.2$ under weak surface anchoring and Hirata *et al.*[7] were able to obtain a stable stripe domain with the periodicity of 250×10^{-4} cm (i.e. $p \simeq 500 \times 10^{-4}$ cm). The relatively small thickness-to-pitch ratio in the present diffusion experiments indicates that, in fact, there exists an additional liquid crystal-surface decoupling effect due to the concentration gradient. The consequent effect of the concentration gradient in reducing the surface anchoring is evident in the P_c–L_c data of figure (5), where the cholesteric pitch value as large as 800×10^{-4} cm and L_c/P_c as small as 0.02 are obtained.

D) Comparison with the theory:

The theoretical model for storage-mode (fingerprint) cholesteric systems has been developed by Luban *et al.*[11] Accordingly, the equilibrium behaviour of the director and the cholesteric pitch as a function of the film thickness ($2L$) and surface energy coefficient (C), as well as the dependence of the critical thickness L_c on C have been established. The result resembling de Gennes calculation in the case of the applied magnetic field (1), has shown that as L is decreased to a critical value L_c, the pitch diverges logarithmically when (L–L_c) approaches zero. Thus the system at $L = L_c$ experiences an induced cholesteric-nematic transition. At the cholesteric-nematic transition, the theory predicts a continuous relation between the reduced critical thickness $\ell_c = 2\pi L_c/P_c$ and the normalized critical pitch denoted as $C = P_c \cdot C/4\pi K_{11}$, where C is the coefficient of the surface energy and K_{11} is the average elastic constant (assuming that $K_{11} = K_{22} = K_{33}$). Notice that in the above relations, Luban *et al.* have used the notation $q_o = 2\pi/\lambda_o$, where $\lambda_o \equiv p_c$ (see also equations 2.16 and 2.21 and figure (*4*) in reference (*11*)). In figure (6) we show portion of ℓ_c vs C plot which has been originally calculated by Luban *et al.* and plotted in their figure (4). The dashed curve is the same plot at the limit range of $C\,\ell \leqslant 0.1$. The quantitative verification of this theory requires a knowledge of the C and K_{11} which are lacking in the present system. On a qualitative basis we, however, made a comparison between our data and the theory. The results of all diffusion experiments are

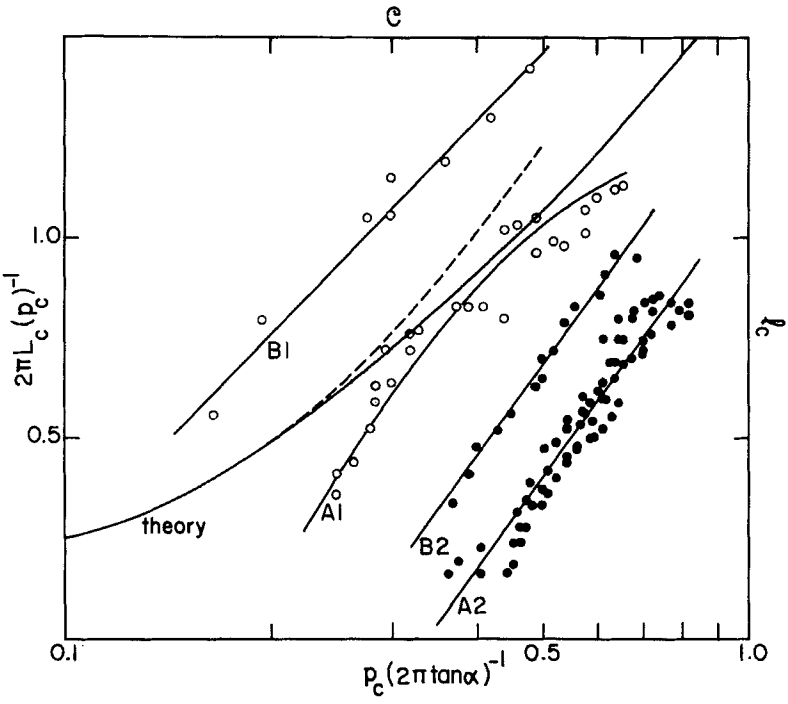

FIGURE 6 Comparison between the present experimental data [$2\pi L_c/P_c$ vs. ln ($P_c/2\pi$ tan (α)] and the Luban *et al.* theory (ℓ_c vs. ln C). Open circles: geometry (1). Dark circles: geometry (2).

presented in figure (6) by $2\pi L_c/P_c$ vs $P_c/2\pi$ tan (α) plots. The ordinate and abscissa are analogous to C_c and ℓ_c of the theory. With the exception of the A1 data, the other results exhibit a qualitative agreement with the theory. The source of the curious behavior of the points in the A1 experiment is not clear. However, an agreement may be established if the upper portion of the data points are ignored. Regardless of this discrepancy, the general characteristics of the experimental data which is within the order of magnitude of the lower portion of the theoretical curve, i.e. ($C\ell_c = CL/K_{11}$) $\lesssim 0.1$, suggest that surface anchoring is weak (small C value). This is a further confirmation of the contribution of the diffusion concentration gradient in reducing the liquid crystal-surface interactions. Further quantitative examination of this theory requires detailed knowledge of the material constant. The coefficient of the surface energy and particularly, if the diffusion study is the experimental approach, the exact quantitative contributions of the concentration and thickness gra-

dients to the P_c–L_c relation are required, which is the task of future investigations.

References

1. P. G. De Gennes, *Solid State Commun.*, **6**, 163 (1968).
2. R. B. Meyer, *Appl. Phys. Lett.*, **12**, 281 (1968).
3. J. J. Wysoḳi, J. Adams and W. Haas, *Phys. Rev. Lett.*, **20**, 1024 (1968).
4. T. B. Harvey, III, *Mol. Cryst. Liq. Cryst.*, **34**, 225 (1977).
5. F. Rondelez and J. P. Hulin, *Solid State Commun.*, **10**, 1009 (1972).
6. F. Rondelez, Ph.D. Thesis, Orsay, France (1973).
7. S. Hirata, T. Alkahane and T. Tako, *Mol. Cryst. Liq. Cryst.*, **75**, 47 (1981).
8. C. G. Lin-Hendel, *J. Appl. Phys.*, **53**, 916 (1982).
9. C. G. Lin-Hendel, *Appl. Phys. Lett.*, **38**, 615 (1981).
10. H. P. Hinov, E. Kukleva and A. I. Derzhanski, *Mol. Cryst. Liq. Cryst.*, **98**, 109 (1983).
11. M. Luban, D. Mukamel and S. Shtrikman, *Phys. Rev. A.*, **10**, 360 (1974).
12. H. Hamkemi and M. M. Labes, *J. Chem. Phys.*, **61**, 4020 (1974).
13. H. Hakemi, *Mol. Cryst. Liq. Cryst.*, (Letts), **82**, 303 (1982).
14. H. Hakemi, *Mol. Cryst. Liq. Cryst.*, **95**, 309 (1983).
15. H. Hakemi and M. M. Labes, *J. Chem. Phys.*, **58**, (1973).
16. H. Hakemi, *Thermochimica Acta*, **53**, 211 (1982).
17. R. Cano, *Bull. Soc. Franc. Mineral Crist.*, **91**, 20 (1968).